JOURNAL OF APPLIED ELECTROCHEMISTRY **27** (1997) 970–974

Service life of $Ti/SnO_2–Sb_2O_5$ anodes

B. CORREA-LOZANO, Ch. COMNINELLIS*, A. DE BATTISTI‡

Institute of Chemical Engineering of the Swiss Federal Institute of Technology, CH-1015 Lausanne, Switzerland

Received 22 July 1996; revised 1 October 1996

The service life of $SnO_2–Sb_2O_5$ coated anodes prepared by the spray pyrolysis technique using Ti or Ti/IrO_2 substrate, was studied under galvanostatic conditions ($100\,mA\,cm^{-2}$ in 1 M H_2SO_4 at 25 °C. The results showed that the presence of an IrO_2 interlayer between the Ti substrate and the SnO_2–Sb_2O_5 coating ($Ti/IrO_2/SnO_2–Sb_2O_5$ anode) strongly increases the service life of the anode. This beneficial action of the IrO_2 interlayer was attributed to its high anodic stability and its isomorphous structure with TiO_2 and SnO_2. Cyclic voltammetry and steady-state polarization curves showed that the electrochemical behaviour of the $Ti/IrO_2/SnO_2–Sb_2O_5$ electrode lies between the behaviour of the Ti/IrO_2 and the $Ti/SnO_2–Sb_2O_5$ electrodes due to incorporation of IrO_2 in the $SnO_2–Sb_2O_5$ coating during its preparation.

1. Introduction

Since the discovery by Beer, nearly 30 years ago [1,2], much work has been done on dimensionally stable anodes (DSA®). Although electrodes based on RuO_2 and TiO_2 are widely used in chlorine-alkali cells, electrodes based on IrO_2 and Ta_2O_5 can be used for oxygen evolution in sulfuric acid media [3–5]. The case of electrodes based on SnO_2 is quite interesting, its role ranging between that of minor component in some DSA® type electrodes and that of main components in $SnO_2–Sb_2O_5$ anodes, of interest in electrochemical treatment of organics for wastewater treatment [6–10].

Preparation of these electrodes by the spray pyrolysis technique and their physicochemical and electrochemical properties were discussed previously in relation to the preparation parameters [11–13]. In the present paper, the research was extended to the service life of $SnO_2–Sb_2O_5$ coatings, directly deposited on titanium substrate ($Ti/SnO_2–Sb_2O_5$ electrode) or after deposition of an IrO_2 interlayer on the titanium substrate ($Ti/IrO_2/ SnO_2–Sb_2O_5$ electrode).

2. Experimental details

The $Ti/SnO_2–Sb_2O_5$ and $Ti/IrO_2/SnO_2–Sb_2O_5$ electrodes ($6\,cm^2$) were prepared by deposition of the $SnO_2–Sb_2O_5$ layer, by the spray pyrolysis technique on Ti, pretreated by sandblasting, then etched in boiling 32% HCl during 30 min, or on Ti/IrO_2 substrate. IrO_2 was deposited on Ti by the thermal deposition technique [4], the loading was varied between 1–10 $g\,m^{-2}$. The scheme of the equipment used is shown in Fig. 1. Details of the preparation method itself are given elsewhere [11–13].

In all cases, the composition of the spray solution was 10 g $SnCl_4–5H_2O$ (Aldrich 24.467–8), 0.2 g $SbCl_3$ (Fluka 10775) in 100 ml of ethanol–HCl mixture and the deposition temperature was 530 °C. The SnO_2–Sb_2O_5 loading has been varied between 5–120 $g\,m^{-2}$. Quasisteady-state polarization curves with *iR* drop correction were carried out with an EG-PAR potentiostat/galvanostat (model 362). Details of the ohmic drop correction setup are described elsewhere [13].

The cyclic voltammetry experiments were carried out using a three electrode cell, Pt was used as a counter electrode and $Hg/Hg_2SO_4 . K_2SO_4$ as a reference electrode. To increase the reproducibility of the polarization measurements, the electrodes were electrochemically preconditioned before use. Preconditioning consisted in polarizing the electrodes for 2 h in 0.5 M H_2SO_4 under anodic current density of $50\,mA\,cm^{-2}$ at 25 °C [13].

The service life test was carried out in a two compartment cell under galvanostatic conditions at $100\,mA\,cm^{-2}$ using Zr cathodes; 1 M H_2SO_4 was used as electrolyte and the working temperature was 25 °C. The anode potential relative to the reference electrode ($Hg/Hg_2SO_4 .\ K_2SO_4$ sat.) was monitored during the service life test. The loss in the electrode weight was also measured during some service life tests.

3. Results and discussion

3.1. *Service life of $Ti/SnO_2–Sb_2O_5$ anodes*

A typical behaviour, in terms of electrode potential as a function of time, is shown in Fig. 2. An induction period of about 2 h can be observed, during which the electrode potential increases by ~1 V then the anode

---

* To whom correspondence should be addressed.

‡ On leave from the Department of Chemistry of the University of Ferrara, Italy.

0021-891X © 1997 Chapman & Hall

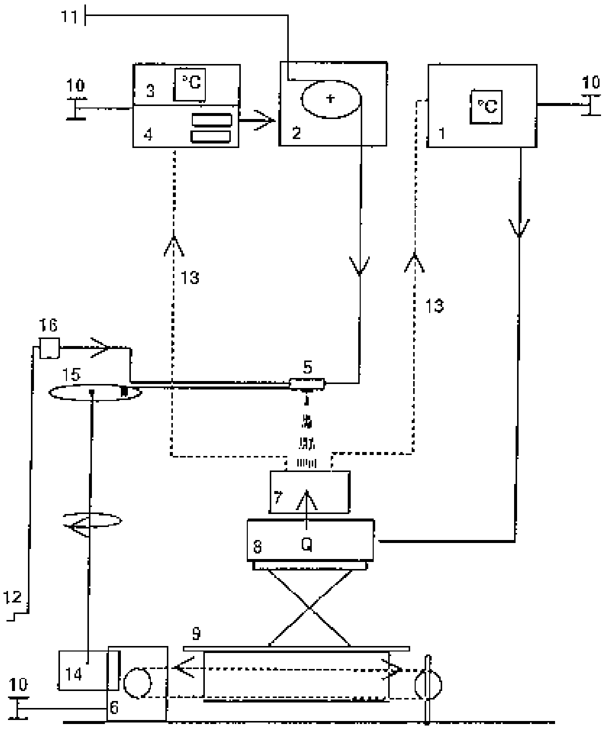

Fig. 1. Setup of spay pyrolysis system. (1) Temperature controller, (2) peristaltic pump, (3) temperature switch, (4) chronometer (effective spraying and total time), (5) spray nozzle, (6) motor for lateral and circular displacement, (7) heating chamber, (8) heating plate, (9) lateral displacement support, (10) electrical connection, (11) spray solution, (12) carrier-gas (N_2), (13) connection to thermocouples, (14) transmission gear, (15) rotating system and nozzle support, and (16) flow-meter for the carrier-gas (N_2).

potential oscillates between 2.5 and 3.6 V (Hg/$Hg_2SO_4 . K_2SO_4$). Finally after about 12 h of electrolysis the anode potential increases steeply, indicating the deactivation of the anode. The electrode service life for the Ti/SnO_2–Sb_2O_5 anodes was defined as the time at which the anode potential reaches a value of 5.0 V(Hg/Hg_2SO_4.K_2SO_4).

Following the weight of the anode coating during the service life test shows that the weight loss of the anode is proportional to the electrolysis time. At the end of the service life, about 80% of the anode coating was corroded.

The observed oscillation (Fig. 2) and the mechanism of electrode deactivation can be explained on the basis of mechanism for oxygen gas evolution in which a certain degree of nonstoichiometry ($SnO_{2\text{-}x}$) is present in as-prepared films as discussed elsewhere [13]. This initial defectiveness involves a larger concentration of catalytically active sites, where the reaction

$$SnO_{(2-x)} + H_2O \rightarrow SnO_{(2-x)}(^{\cdot}OH) + H^+ + e^- \tag{1}$$

takes place with formation of adsorbed hydroxyl radicals $^{\cdot}OH$. A further oxidation may take place with an increase in oxygen stoichiometry, which however, at this stage, is still below 2:

$$SnO_{(2-x)}(^{\cdot}OH) \rightarrow SnO_{(2-x+y)} + yH^+ + ye^- \tag{2}$$

This modification of the anode surface increases the internal stress of the oxidized layer resulting finally in its detachment. Underlying substoichiometric layers are then exposed to the electrolyte and undergo electrochemical oxidation through the above steps (Equations 1 and 2). This explains the periodical potential oscillations (shown in Fig. 2) and the progressive layer by layer electrode disintegration. The same behaviour was observed for coating prepared under different conditions. However, parameters like deposition temperature and oxide loading strongly influence the service life of the anode.

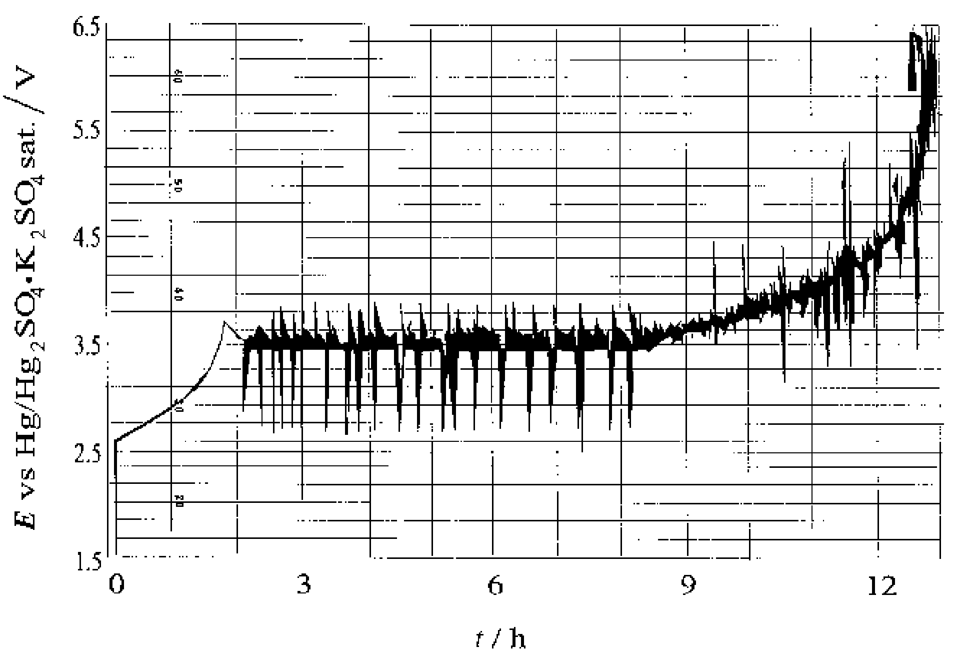

Fig. 2. Service life test for the Ti/SnO_2–Sb_2O_5 electrode. Anode potential as a function of electrolysis time. Electrolyte: 1 m H_2SO_4; $i = 100\,mA\,cm^{-2}$, $T = 25\,°C$.

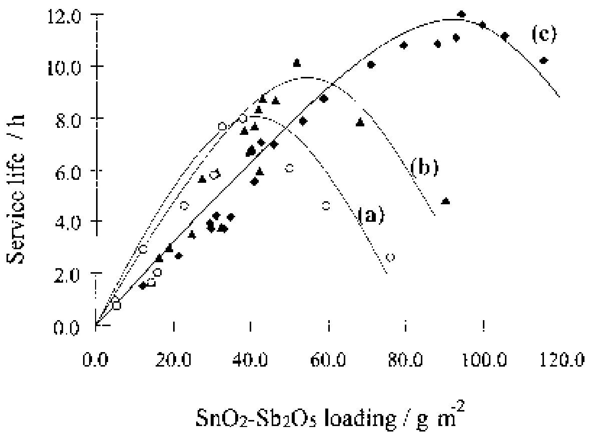

Fig. 3. Service life of the $Ti/SnO_2–Sb_2O_5$ electrode prepared at different temperatures as a function of the $SnO_2–Sb_2O_5$ loading. Electrolyte: 1 m H_2SO_4; $i = 100\,mA\,cm^{-2}$; $T = 25\,°C$. (a) 450 °C, (b)500 °C and (c) 550 °C.

As shown in Fig. 3 for a given preparation temperature, the electrode service life initially increases with the oxide loading, reaching a maximum, and then decreases with oxide loading. The initial increase in service life with oxide loading can be explained by the proposed deactivation mechanism in which the coating is detached layer by layer, which means that the thicker the coating the higher the service life; this is the case for coating loading below a critical value which depends on the deposition temperature (Fig. 3). The decrease in service life for loading above the critical value can be explained by the presence of a mechanical stress in the coating generated by the difference in thermal expansion between the coating and the Ti base metal.

The shift of the maximum with the preparation temperature (Fig. 3) is probably due to the decrease in crystallite size of the coating with increasing deposition temperature [11, 12] resulting in a decrease in the mechanical stress for a given loading.

The results given in Fig. 3 show that the service life of the $Ti/SnO_2–Sb_2O_5$ anode can be improved using high electrode loading (~100 g m^{-2}) and preparing the electrodes at 550 °C, however the service life remains low for practical application.

3.2. *Service life of $Ti/IrO_2/SnO_2$-Sb_2O_5 anodes*

In an effort to increase the service life of the SnO_2 based anodes, an interlayer of IrO_2 was deposited between the Ti base and the $SnO_2–Sb_2O_5$ coating. The IrO_2 interlayer can benefit the service life of the SnO_2 based anodes due to its high anodic stability and its isomorphous structure with TiO_2 and SnO_2. A typical anode potential–time curve for the $Ti/IrO_2/SnO_2–Sb_2O_5$ electrode obtained during the service life test at 100 mA cm^{-2} in 1 M H_2SO_4 is shown in Fig. 4. As for the $Ti/SnO_2–Sb_2O_5$ electrode, an induction period is observed during which the electrode potential increases slowly to reach steady state after about 50 h. After this induction period the anode potential remains constant for a long period (~900 h) and there is no oscillation of potential (as was the case with the $Ti/SnO_2–Sb_2O_5$ electrode). Finally, the electrode potential decreases to a value which corresponds to the Ti/IrO_2 electrode. The service life of the $Ti/IrO_2/SnO_2–Sb_2O_5$ electrode has been defined as the time at which the anode potential corresponds to the potential of the Ti/IrO_2 electrode. At the end of the service life of this electrode the electrode looses about 70% of the $SnO_2–Sb_2O_5$ coating. It is interesting to note that the anode potential of the $Ti/IrO_2/SnO_2–Sb_2O_5$ electrode during the service life test (Fig. 4) is much lower than the anode potential of the $Ti/SnO_2–Sb_2O_5$ electrode.

Figure 5 shows the influence of the coating loading on the service life of the $Ti/IrO_2/SnO_2–Sb_2O_5$ electrode, the decrease in service life observed at high loading (> 80 g m^{-2}) can be explained by the presence of a residual mechanical stress generated by the difference in thermal expansion between the coating and the base metal. The low stability observed at high

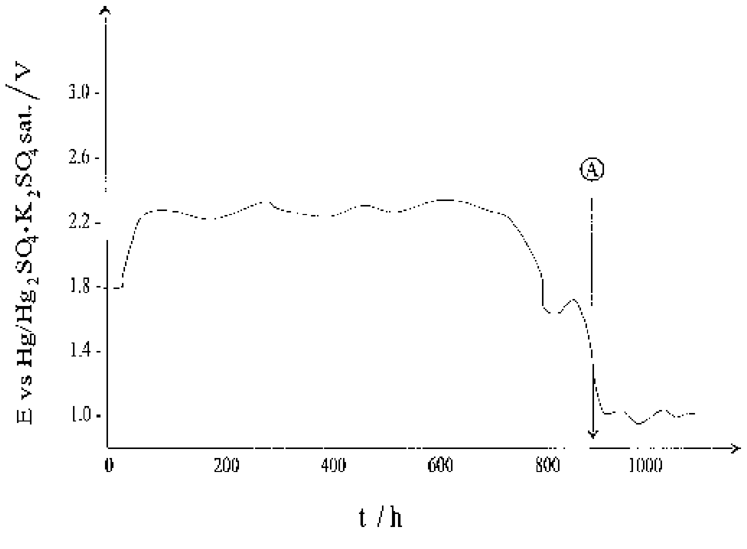

Fig. 4. Service life test for the $Ti/IrO_2/SnO_2–Sb_2O_5$ electrode. Electrolyte: 1 m H_2SO_4; $i = 100\,mA\,cm^{-2}$, $T = 25\,°C$. IrO_2 interlayer loading: 10 g m^{-2}, $SnO_2–Sb_2O_5$ loading: 30 g m^{-2}. Ⓐ: End of service life test.

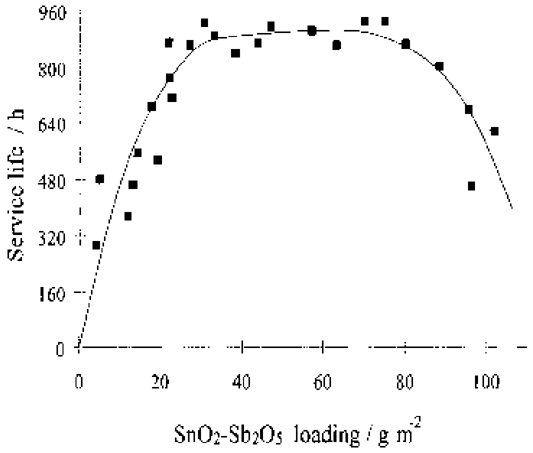

Fig. 5. Service life of the Ti/IrO$_2$/SnO$_2$–Sb$_2$O$_5$ electrode prepared at 530 °C as a function of the SnO$_2$–Sb$_2$O$_5$ loading. Interlayer IrO$_2$ loading: $10\,g\,m^{-2}$. Electrolyte: 1 m H$_2$SO$_4$; $i = 100\,mA\,cm^{-2}$, $T = 25\,°C$.

loading is not specific to this type of coating but is a general feature of the DSA type electrodes.

To better understand the increase in service life (by about two orders of magnitude) and the low anode potential (by about 1 V) of the SnO$_2$–Sb$_2$O$_5$ coating in the presence of an IrO$_2$ interlayer, cyclic voltammetry and steady state polarization measurements were carried out. The results were compared with those for Ti/IrO$_2$ and the Ti/SnO$_2$–Sb$_2$O$_5$ electrodes. In Fig. 6 cyclic voltammograms (CV) obtained in 0.5 M H$_2$SO$_4$ at 25 °C are shown for the different electrodes studied. The Ti/SnO$_2$–Sb$_2$O$_5$ electrodes are characterized by a small voltammetric charge q^* in comparison to the Ti/IrO$_2$ electrode. The small q^* obtained for the Ti/SnO$_2$–Sb$_2$O$_5$ electrode may be attributed to the low porosity of the SnO$_2$–Sb$_2$O$_5$ coating. In fact, film thickness measurements have shown that the measured density of the coating ($\rho = 6.7\,g\,cm^{-3}$) is close to that of crystalline SnO$_2$ ($\rho = 6.95\,g\,cm^{-3}$). This implies that the coating is compact and essentially nonporous [11,12]. SEM images for SnO$_2$–Sb$_2$O$_5$ and IrO$_2$ coatings on Ti substrate (Fig. 7) show that the IrO$_2$ coating, which was prepared by the thermal decomposition technique, is much more porous than the SnO$_2$–Sb$_2$O$_5$ coating which was prepared by the spray pyrolysis technique. The obtained morphology for the SnO$_2$–Sb$_2$O$_5$ coating is not specific to this type of coating but is related to the preparation technique. In fact, the spray pyrolysis technique in which the formation of the coating is carried out in a gas-phase reaction is characterized by the formation of a crystalline and compact coating [11, 12]. In the presence of an IrO$_2$ interlayer the voltammetric charge q^* increases and its shape is similar to that obtained with the Ti/IrO$_2$ electrode (Fig. 6). This indicates that IrO$_2$ is incorporated in the SnO$_2$–Sb$_2$O$_5$ coating by diffusion during the coating preparation.

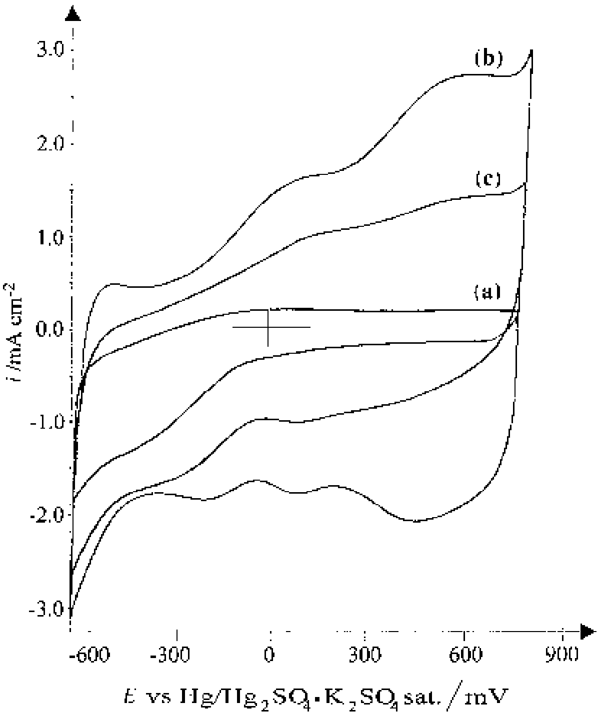

Fig. 6. Cyclic voltammograms obtained in 0.5 m H$_2$SO$_4$ at 25 °C, scan rate: $50\,mV\,s^{-1}$. (a) Ti/SnO$_2$–Sb$_2$O$_5$ electrode (loading: $30\,g\,m^{-2}$); (b) Ti/IrO$_2$ electrode (loading: $5\,g\,m^{-2}$); (c) Ti/IrO$_2$ ($5\,g\,m^{-2}$)/SnO$_2$–Sb$_2$O$_5$ ($30\,g\,m^{-2}$).

Tafel plots, with iR drop correction, for oxygen evolution in 0.5 M H$_2$SO$_4$ at 25 °C for the Ti/IrO$_2$/SnO$_2$–Sb$_2$O$_5$ electrodes, with a constant IrO$_2$ inter-

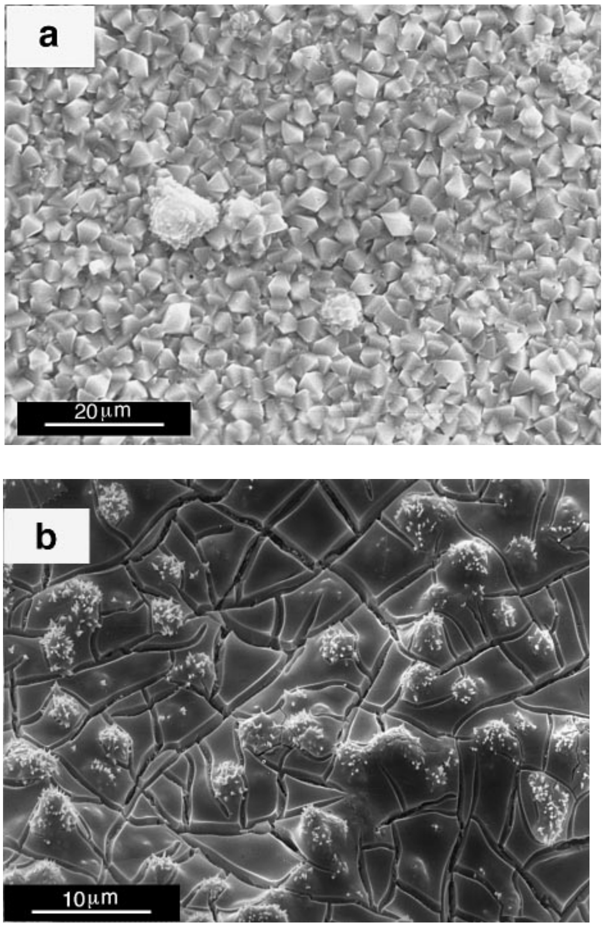

Fig. 7. SEM images of (a) Ti/SnO$_2$–Sb$_2$O$_5$ and (b) Ti/IrO$_2$.

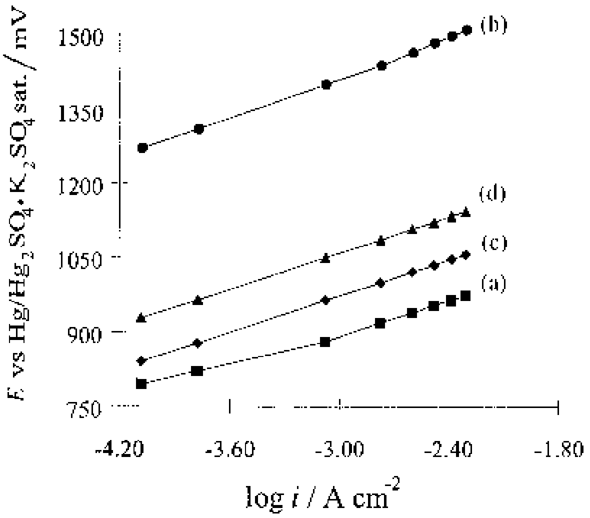

Fig. 8. Tafel plots for oxygen evolution at: (a) Ti/IrO_2 (10 g m^{-2}); (b) Ti/SnO_2–Sb_2O_5 (30 g m^{-2}); (c) Ti/IrO_2 (10 g m^{-2})/SnO_2–Sb_2O_5 (10 g m^{-2}); (d) Ti/IrO_2 (10 g m^{-2})/SnO_2–Sb_2O_5 (30 g m^{-2}).

layer loading (10 g m^{-2}) for various SnO_2–Sb_2O_5 coatings are shown in Fig. 8. In the same figure, Tafel plots for the Ti/IrO_2 and Ti/SnO_2–Sb_2O_5 electrodes are given. The Ti/SnO_2–Sb_2O_5 electrodes are characterized by a high oxygen evolution overpotential and follow the Tafel relation, with a slope at 0.12 V decade^{-1}. For the Ti/IrO_2 electrode, a lower Tafel slope, 0.070 V decade^{-1} is found at low current densities and 0.12 V decade^{-1} at high current densities.

As shown in Fig. 8, the behaviour of the Ti/IrO_2/SnO_2–Sb_2O_5 electrodes lies between the behaviour of the Ti/IrO_2 and the Ti/SnO_2–Sb_2O_5 electrodes. Increasing the SnO_2–Sb_2O_5 loading for a given interlayer loading (10 g m^{-1}), results in a shift in the Tafel line towards the Ti/SnO_2–Sb_2O_5 electrode increasing the oxygen gas evolution overpotential.

Figure 9 shows polarization curves for oxygen evolution in 0.5 M H_2SO_4 for electrodes with a constant SnO_2–Sb_2O_5 loading (30 g m^{-2}) and for various IrO_2 interlayers. For comparison, the Ti/IrO_2 and Ti/SnO_2–Sb_2O_5 electrodes are given. This figure shows that increasing the IrO_2 interlayer loading for a given SnO_2–Sb_2O_5 loading results in a shift of the polarization curve towards the Ti/IrO_2 electrode decreasing the oxygen evolution overpotential. This is another indication that the IrO_2 is incorporated in the SnO_2–Sb_2O_5 coating by diffusion of the IrO_2 towards the SnO_2–Sb_2O_5 coating during its preparation.

The behaviour of the Ti/IrO_2/SnO_2–Sb_2O_5 anodes towards the electrochemical oxidation of phenol, a model pollutant for wastewater treatment, is now under investigation [14].

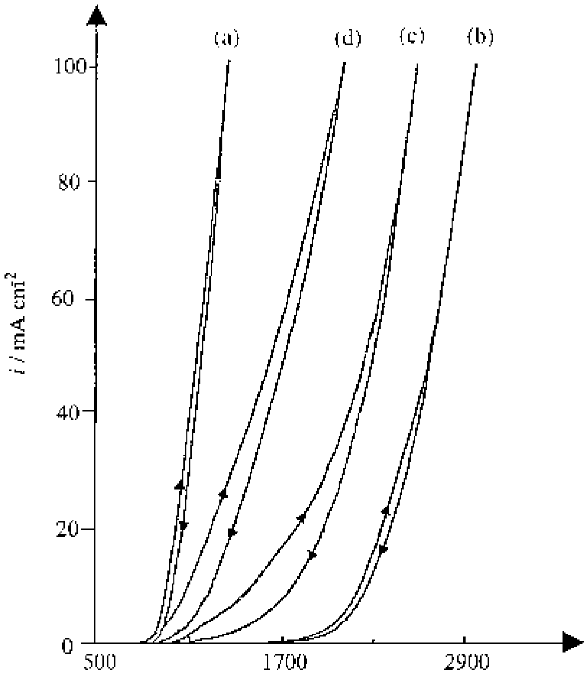

Fig. 9. Polarization curves for oxygen evolution in 0.5 m H_2SO_4 at 25 °C; scan rate: 10 mV s^{-1}. (a) Ti/IrO_2 (5 g m^{-2}); (b) Ti/ SnO_2–Sb_2O_5 (30 g m^{-2}); (c) Ti/IrO_2 (1.4 g m^{-2}) / SnO_2–Sb_2O_5 (30 g m^{-2}); (d) Ti/IrO_2 (5 g m^{-2})/SnO_2–Sb_2O_5 (30 g m^{-2}).

References

[1] H.B. Beer, *Neth.Appl. 6 606 302* (1966) and *US Patent 3 632 498 (1972).*
[2] O. De Nora, A. Nidola, G. Trisoglio and G. Bianchi, *British Patent 1 399 576* (1973).
[3] J. Rolewicz, Ch. Comninellis, E. Plattner and J. Hinden, *Electrochim. Acta* **33** (1988) 573.
[4] G. P. Vercesi, J.- Y. Salamin and Ch. Comninellis, *ibid.* **36** (1991) 991.
[5] Ch. Comninellis and G. P. Vercesi, *J. Appl. Electrochem.* **21** (1991) 136.
[6] S. Stucki, R. Kötz, B. Carter and W. Suter, *ibid.* **21** (1991) 99.
[7] Ch. Comninellis and C. Pulgarin, *ibid.* **23** (1993) 108.
[8] Ch. Comninellis, *Electrochim. Acta* **39** (1994) 1857.
[9] Ch. Comninellis and A. Nerini, *J. Appl. Electrochem.* **25** (1995) 23.
[10] Ch. Comninellis and A. De Battisti, *J.Chim.Phys.* **93** (1996) 673.
[11] B. Correa-Lozano, Ch. Comninellis and A. De Battisti, *J. Appl. Electrochem.* **26** (1996) 83.
[12] Idem, *J.Electrochem. Soc.* **146** (1996) 203.
[13] Idem, J.*Appl. Electrochem.* **26** (1996) 683.
[14] B. Correa-Lozano and Ch. Comninellis, *J. Appl. Electrochem.*, in preparation.